2014 International Conference on Unmanned Aircraft Systems (ICUAS)
May 27-30, 2014. Orlando, FL, USA

Valve Turning using a Dual-Arm Aerial Manipulator

Matko Orsag, Christopher Korpela, Stjepan Bogdan, and Paul Oh

Abstract— **This paper presents a framework for valve turning using an aerial vehicle endowed with dual multi-degree of freedom manipulators. A tightly integrated control scheme between the aircraft and manipulators is mandated for tasks requiring aircraft to environmental coupling. An analysis of yaw angle dynamics is conducted and implemented into the controller. A human machine interface provides user input to actuate the manipulators, become coupled to the valve, and perform the turning operation. We present recent results validating the valve turning framework using the proposed aircraft-arm system.**

I. Introduction

Valve turning represents a classic controls problem along with insertion tasks and tool usage. The ground robotics community has largely solved these problems. There are many examples of door opening, using a drill, assembly of structures, and inserting a power plug by ground vehicles with one or more dexterous arms. Many of these tasks require position and/or force control and typical implementations involve force/torque sensing, vision systems, or a combination of these methods. The ground-based system must coordinate the vehicle and arm motions to perform these tasks. While the coupling between the environment (i.e. valve, knob, handle) and robot does influence the vehicle base with added contact forces/torques and friction, the base can typically maintain stability during the entire motion.

However, the strong coupling required during valve or knob turning greatly influences the dynamics of an aerial manipulator. Rigidity in the manipulator and the propagation of contact forces when interacting with the environment can cause crashes. There have been recent results where multi-DOF aerial manipulators have experienced coupling with the environment [1]–[4]. Other groups have investigated compliance in assembly tasks [5]–[7], or dynamic stability and control w.r.t. center of mass and moment of inertia variations [8]–[10].

Manuscript received February 17, 2014. This work was supported in part by the Air Force Research Laboratory, under agreement number FA8655-13-1-3055, the National Science Foundation (NSF) award CNS-1205490, and the European Community Seventh Framework Program under grant No. 285939 (ACROSS). The U.S. Government is authorized to reproduce and distribute reprints for Governmental purposes not withstanding any copyright notation thereon. The views and conclusions contained herein are those of the authors and should not be interpreted as necessarily representing the official policies or endorsements, either expressed or implied, of the Air Force Research Laboratory, the U.S. Government, or the NSF.

M. Orsag and S. Bogdan are with the Faculty of Electrical Engineering and Computing, University of Zagreb, 10000 Zagreb, Croatia morsag@fer.hr,sbogdan@fer.hr

C. Korpela and P. Oh are with the Drexel Autonomous Systems Lab, Drexel University, Philadelphia, PA 19104 USA cmk325@drexel.edu, paul@coe.drexel.edu

Fig. 1. MM-UAV dual-armed system performing a valve turning task.

This paper presents a solution to the valve turning problem from an aerial vehicle using dual 2-DOF manipulators, dubbed MM-UAV (Mobile Manipulating Unmanned Aerial Vehicle). A control scheme to coordinate the coupled manipulator-aircraft system (Fig. 1) is implemented to allow for the strong coupling between the manipulators and environment. Section II briefly describes the theory behind valve turning tasks and the algorithm used for detection. Section III details the kinematic and dynamic model for the aircraft and manipulators. In Section IV, we disseminate on the proposed hardware infrastructure, as well as the proposed human-machine interface (HMI). Finally, we present the results of valve turning experiments in Section V and conclude the paper proposing further developments and future plans.

II. The Valve Turning Problem

Valve, knob, and handle turning has been widely studied for use with industrial robots, mobile manipulators, and personal assistance robots. A typical requirement involves a grasp and turn of an object that remains fixed to the environment but allowed to rotate. Our framework and solution will be evaluated by performing valve turning, which is one of the tasks required for the recent DARPA Robotics Challenge (DRC) [11]. The task requires a robot to locate, approach, grasp, and turn an industrial valve with two hands. Valve turning presents a challenging test-case for any system due to the perception and dexterous manipulation required [12]. While a ground robot can approach a value and become physically coupled to it, a flying robot with one or more manipulators faces far greater difficulties. The direct coupling between the manipulators and valve can cause sudden unexpected changes in the vehicle dynamics. The aerial manipulator must constantly adjust to compensate for the vehicle movement and further have adequate compliance

to prevent a crash, particularly during the manipulator-environment coupling after grasping and while turning.

Valves are found in virtually every industrial process including water and sewage processing, mining, power generation, processing of oil, gas and petroleum, food manufacturing, chemical and plastic manufacturing, and many other fields. Therefore, it is easy to imagine a disaster scenario where it is necessary to deploy an aerial robot to close a crucial valve and thus prevent further human casualties or damage. Unlike humanoid or mobile robots, closing a valve for an aerial robot is a highly complicated task which requires a robot to: Locate the handle, Land on the handle, Grab on to the handle and finally Twist the handle, using the aircraft's own degrees of freedom.

In industrial pipelines, different valves for gas, water, oxygen and many other gases and fluids are color coated [13]. Although standards vary from country to country and industry to industry, some consistencies in standards have risen.

According to most standards, a good practice for piping systems which do not require warning colors is to paint them to differ from their surroundings. For humans, the use of these standards promotes safety and lessens chances of error in times of an emergency by providing a uniform color code to quickly warn personnel of outstanding hazards inherent in the materials involved. On the other hand, for robots, these standards insure an additional color filter layer in camera-based vision feedback algorithms. Given specific mission requirements (i.e. fire, pollution, or human safety), a robot can easily spot a specific valve using a color filter in order to separate it from its surroundings. In practical applications, a single industrial pipeline system consists of various types of valves. The handwheel shape is ideally designed for the envisioned scenario: the aircraft grabs onto the valve handle and twists it using its own degrees of freedom. Although other shapes could be engaged as well because it is possible to land on them, they fall out of the scope of the proposed scenario.

There are two distinctive features of a handwheel handle design. The first concerns the circular shape of its outer rim that enables one to deploy some type of circle or ellipse detection algorithm. Varying in number from handle to handle are two, three, or more spokes that connect the circular rim with the handle hub. These spokes form lines that cross each other at the center of the handle, i.e. the hub. Using line detection algorithms, such as a Hough transform, it is possible to utilize this second distinctive handwheel feature.

III. Aerial Manipulator Model

At present, aerial robot dynamics and kinematics are widely understood [10], [14], [15]. During the course of this research we went through several prototype designs, each tailored for a specific task (i.e. peg-in-hole, pick and place, etc). The same methodologies apply for the valve turning mission. Ideally, one strives to accomplish a single manipulator design suitable for all the tasks, like the one shown in Fig. 2, but due to payload constraints it is not yet possible to accomplish this goal. Therefore, the proposed kinematic chain, with two selected degrees of freedom (DOF), suitable for this mission is described with Denavit-Hartenberg parameters given in Table I and shown in Fig. 3. The manipulators (noted as arms A and B with links L_i) are symmetrical and attached below the center of gravity of the quadrotor frame and equally offset from the vehicle's geometric center.

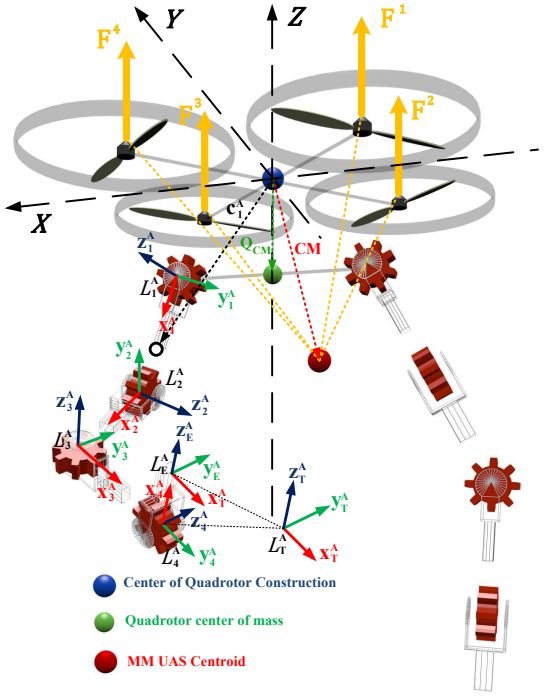

Fig. 2. Proposed UAS model showing quadrotor and manipulators (links expanded for clarity). 4 DOFs are shown for each arm to indicate a complete arm design [16].

A. Valve approach kinematic constraints

In order for a 2 arm manipulator to grab the valve and remain symmetric with respect to the UAS ZY plane, certain kinematic constraints on joint movements need to be applied. Given a desired vertical distance $H(q_1, q_2)$ along the z axis, and horizontal distance $X(q_1, q_2)$ along the x axis of the body frame, one yields the following constraints on joint movements:

$$q_1 = \pm acos\left[\frac{{L_2}^2 - H(q_1,q_2)^2 - X(q_1,q_2)^2 - {L_1}^2}{2L_1\sqrt{H(q_1,q_2)^2 + X(q_1,q_2)^2}}\right] \quad (1)$$

$$q_2 = \pm acos\left[\frac{H(q_1,q_2)^2 + X(q_1,q_2)^2 - {L_1}^2 - {L_2}^2}{2L_1 H(q_1,q_2) X(q_1,q_2)}\right] \quad (2)$$

In the previous equations, we omitted indices A and B for left and right part of the system respectively, because in order to maintain symmetry, both manipulators need to move in exactly the same way (i.e. $q_1^A = -q_1^B$, $q_2^A = -q_2^B$). Lengths L_1 and L_2 denote link sizes from DH parameters in Table I.

B. Aerial manipulator dynamics

Complete dynamic model of the system can be derived through one of the classical dynamic analysis methods like Newton or Lagrange-Euler [17], [18]. No matter what method is chosen, the end result is a matrix equation of the following form:

$$\mathbf{D}(\boldsymbol{\xi})\ddot{\boldsymbol{\xi}} + \mathbf{c}(\boldsymbol{\xi}, \dot{\boldsymbol{\xi}}) + \mathbf{h}(\boldsymbol{\xi}) + \mathbf{b}(\dot{\boldsymbol{\xi}}) = \boldsymbol{\tau} \tag{3}$$

where $\mathbf{D}$, $\mathbf{c}$, $\mathbf{h}$, $\mathbf{b}$ represent nonlinear matrices of inertial, centrifugal, gravitational and drag forces, respectively. Vector $\boldsymbol{\eta}$ denotes a $(2n+3) \times 1$ value space, with n being the number of joints defined in joint vector $\mathbf{q}$ $2n \times 1$ space, with an additional 3 degrees of freedom for aircraft attitude control $[\psi, \theta, \phi]$. Torque τ is the input torque combined from manipulator and quadrotor components $[\boldsymbol{\tau}, \boldsymbol{\tau_Q}]$. The rigid body dynamics of rotorcraft are well understood [19], [20], and resemble the form in (3). The quadrotor torque $\boldsymbol{\tau_Q}$ is produced within its propulsion system and takes the following mathematical form:

$$\vec{\boldsymbol{\tau}}_Q(u, \mathbf{q}) = \sum_{i=1}^{4} \vec{\mathbf{Q}}(u)^i + \Delta\vec{\mathbf{CM}}(\mathbf{q}) \times \vec{\mathbf{F}}(u)^i. \tag{4}$$

Much of the previous work in quadrotor control assumes the geometric center and quadrotor center of mass are coincident. With the introduction of two manipulators used for valve turning, the center of mass shifts and the inertia properties change based on arm joint angles and environmental contact forces and torques. The torques and forces produced from the quadrotor propellers have to be taken into account. The torque vector $\vec{\tau}^i$ has two components, one coming from the actual propeller drag Q, and the other due to the displacement of the propeller from the center of mass $\Delta\vec{\mathbf{CM}}(\mathbf{q})$. Equation (4) is valid if we assume symmetric construction and propeller placement. In an aerial manipulator system, the center of mass shifts as each joint (q_j) of the manipulator rotates and the torque becomes a nonlinear function of the manipulator joint angles [16]:

$$\vec{\mathbf{CM}}(\mathbf{q}) = \frac{\vec{\mathbf{Q}}_{cm} m_Q + m_L \sum_{i=1}^{4} [\vec{\mathbf{c}}_i(\mathbf{q})]}{m_Q + 4m_L} \tag{5}$$

Symbols m_Q and m_L denote quadrotor and link respective masses. The same coupling is exhibited for moments of inertia. Combining parallel axis theorem together with axes rotation yields:

$$\mathbf{J}_{UAS} = \sum \mathbf{J}_L^i|_B + m_L \left[(\vec{\mathbf{c}}_i \cdot \vec{\mathbf{c}}_i)\, \mathbf{I} - \vec{\mathbf{c}}_i \otimes \vec{\mathbf{c}}_i \right] \tag{6}$$

where $\vec{\mathbf{c}^i}$ and $\mathbf{J}_L^i|_B$ represent the vector distance from each body part center of mass to the center of construction, and moment of inertia (observing aircraft body as a part of the kinematic chain, with its own centroid distance and moment of inertia). $\mathbf{I}$ denotes a 3×3 identity matrix, and $\otimes$ represent the outer product of the two vectors.

In our previous work we analyzed overall stability of a flying aerial manipulator. In this paper however, we focus on yaw angle dynamics since it is the most important for the envisioned valve turning scenario. Moreover, due to coupling between the environment (i.e. valve) and aerial manipulator, yaw angle dynamics is regarded crucial for aircraft stability.

TABLE I

DENAVIT-HARTENBERG PARAMETERS FOR MANIPULATOR

Link Number	θ (rad.)	d (mm)	a (mm)	α (rad.)
1	q_1	0	L_1	0
2	q_2	0	L_2	0

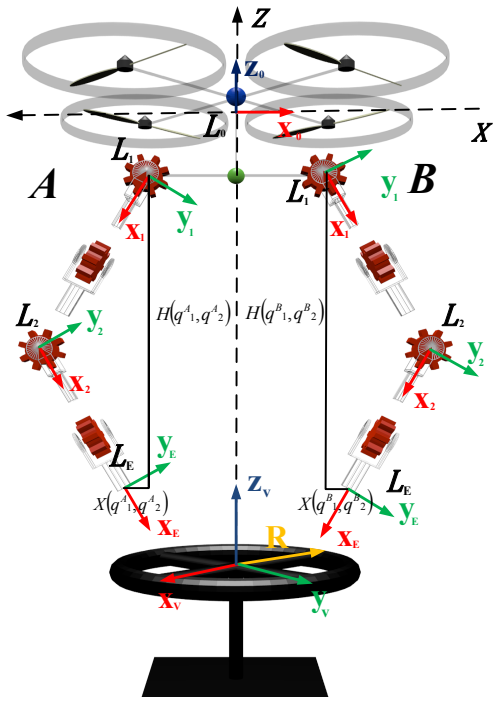

Fig. 3. Coordinate system for valve turning approach.

C. Yaw angle dynamics

Confining the dynamic analysis to yaw angle dynamics, we write quadrotor body dynamics equations for yaw angle attitude control:

$$I_{zz}(\vec{\mathbf{q}})\dot{\omega}_z = \left(I_{xx}(\vec{\mathbf{q}}) - I_{yy}(\vec{\mathbf{q}})\right)\dot{\omega}_x\dot{\omega}_y + \beta(\omega_z) + \vec{\tau}_z^C + \vec{\tau}_z^A \tag{7}$$

$$\vec{\tau}_z^C = (\tau_z^1 - \tau_z^2 + \tau_z^3 - \tau_z^4)\hat{z} \tag{8}$$

The aim for aerial manipulation tasks is to keep the aircraft steady, with a minimum amount of motion, which is usually constrained to only one direction (i.e. x or y). This assumption minimizes the effect dynamic coupling $\left(I_{xx}(\vec{\mathbf{q}}) - I_{yy}(\vec{\mathbf{q}})\right)\dot{\omega}_x\dot{\omega}_y$ has on yaw angle dynamics. Also, by keeping the manipulator motion slow with respect to the quadrotor attitude motion, the dynamic coupling between UAS body and arm torques $\vec{\tau}_z^A$ is minimized.

Next, model simplification comes from the fact that the payload limits joint actuator choice, so the manipulators need to be constructed using lightweight servo motors. These kind

of servo motors often offer little or no choice for control parametrization. Thus the dynamics of the manipulators has to be modeled as a position control closed loop system. However, suitable servo motors can be selected so that the variations of the closed loop dynamics can be minimized and regarded as constant. Decoupling manipulator dynamics from the body motion and approximating closed loop dynamics with a second order transfer function, one can write the state space model of the manipulator part of the system:

$$\begin{bmatrix} \dot{q}_1 \\ \ddot{q}_1 \\ \\ \vdots \\ \\ \dot{q}_{2n} \\ \ddot{q}_{2n} \end{bmatrix} = \begin{bmatrix} 0 & 1 & 0 & \dots & 0 & 0 & 0 \\ -\frac{1}{{\omega_1}^2} & -\frac{2\zeta_1}{\omega_1} & 0 & \dots & 0 & 0 & 0 \\ 0 & 0 & 0 & \dots & 0 & 0 & 0 \\ \vdots & \vdots & \vdots & \ddots & \vdots & \vdots & \vdots \\ 0 & 0 & 0 & \dots & 0 & 0 & 0 \\ 0 & 0 & 0 & \dots & 0 & 0 & 1 \\ 0 & 0 & 0 & \dots & 0 & -\frac{1}{{\omega_{2n}}^2} & -\frac{2\zeta_{2n}}{\omega_{2n}} \end{bmatrix} \begin{bmatrix} q_1 \\ \dot{q}_1 \\ \\ \vdots \\ \\ q_{2n} \\ \dot{q}_{2n} \end{bmatrix} + \begin{bmatrix} 0 \\ u_1 \\ \\ \vdots \\ \\ 0 \\ u_{2n} \end{bmatrix} \tag{9}$$

where each joint has specific dynamics (i.e. natural frequency ω_i and damping ζ_i), $u_i = \frac{1}{{\omega_i}^2} qr_i$ where qr_i defines control input for the i-th joint. Combining joint dynamics with body dynamics yields a state space dynamic representation of the system shown in Fig 4. The system can be written in matrix form:

$$\begin{bmatrix} \dot{\phi} \\ \dot{\omega_z} \\ \dot{\mathbf{q}} \end{bmatrix} = \begin{bmatrix} 0 & 1 & \mathbf{c}^{\phi}(\boldsymbol{\xi}, \dot{\boldsymbol{\xi}}) \\ 0 & -\beta(\omega_z) & \\ & \mathbf{0} & A_q \end{bmatrix} \begin{bmatrix} \phi \\ \omega_z \\ \mathbf{q} \end{bmatrix} + \begin{bmatrix} 0 \\ \phi_r \\ \mathbf{u}_q \end{bmatrix} \tag{10}$$

where $\mathbf{c}^{\phi}(\boldsymbol{\xi}, \dot{\boldsymbol{\xi}})$ denotes a $2n \times 2$ matrix of Coriolis and centrifugal forces in (3), produced on the UAS body coming from joint movements of manipulators.

D. Valve interaction coupling

We consider valve turning tasks to be strongly coupled events where the aerial manipulator must achieve contact forces and torques capable of turning a valve and holding on to it at the same time. In contrast, a pick and place or insertion task only requires a brief moment of loose coupling with the ground during the grasp or insertion.

Once the aircraft-arm system has taken position over the valve and the geometric center of the valve is aligned with the aerial system centroid as shown in Fig. 3, we can assume that the valve is constrained on a plane parallel to the bottom plate of the quadrotor. In this situation the quadrotor center of mass is positioned directly above the pivot of the valve. We assume that the valve is 'perfectly' balanced, that is the pivot of the valve represents the center of mass in the plane on which the valve turns. As the arms are symmetric and articulate equally and opposite of each other, the combined arms' center of mass shifts only along the z axis of the quadrotor geometric center. A constrained grab, when the quadrotor arms come into contact with the valve and clamp on, changes the overall center of mass (5) to include valve mass m_V and distance from the center of construction $\mathbf{c}(H, X)$:

$$\vec{\mathbf{CM}}(\mathbf{q}) = \frac{\vec{\mathbf{Q}}_{cm} m_Q + (\mathbf{c}^*(H, X)) m_V + m_L \sum_{i=1}^{4} [\vec{\mathbf{c}}_i(\mathbf{q})]}{m_Q + m_V + 4m_L} \tag{11}$$

It is worth noting that $\mathbf{c}^*(H, X) = \mathbf{c}(H, X) + R$ is a function of commanded manipulator positions X and H and valve radius R. Furthermore, it is important to view the valve as a static object in the environment with respect to all degrees of freedom, except yaw angle. Due to the limitations in aircraft size and power, it can only turn the valve, but not tilt it or change its position. Mathematically, this is achieved for, $\lim_{m_v \to \inf} \vec{\mathbf{CM}}(\mathbf{q}) = \mathbf{c}(H, X)$, which makes $\mathbf{c}(H, X) + R$ an anchor point for the coupled system. In the quadrotor body frame, the anchor point is located at $[0, 0, -H]$. The same mathematical analysis can be applied for coupled moments of inertia. That is, moments of inertia become infinity large along the x and y axes. Putting it all together, the aircraft rotates the valve around its z_V axis, which is aligned with body z_B axis, while the rest of the dynamics is tightly coupled to the environment.

For this case, the quadrotor propulsion system acts as a torque controlled joint. Reusing assumptions from previous paragraph, equation (4) still holds for the coupled system. Moment of inertia is discretely changed accounting for additional valve moment of inertia in z axis (i.e. $I^{valve} = m_V R^2$ with R as valve radius in Fig. 3), so that the total inertia of quadrotor, arm, valve system becomes:

$$I_{total} = I^{quad} + \sum_{i=1}^{i=n} I_i^{arm} + I^{valve} \tag{12}$$

Another discrete change of system dynamics comes from valve friction. Unlike in-air motion, when the UAS is tightly coupled with the valve, it exhibits friction forces produced within valve turning mechanism. Aerodynamic drag is thus replaced with a complex nonlinear force that is difficult to model accurately, but it has significant effect on UAS actuators. Valve turning friction has three distinct components, modeled with following function [21]:

$$b_k(\omega_z) = b_k^v \omega_z + sgn(\omega_z) \left[b_k^d + (b_k^s - b_k^d) e^{\frac{-|\omega_z|}{\epsilon}} \right] \tag{13}$$

- b_k^v represents viscous friction, much like linearized aerodynamic drag β
- b_k^d is dynamic friction coefficient
- b_k^s stands for static friction, which needs to be overcome in order to start turning the valve.

E. Valve turning as switching system

Since the previous analysis shows that valve turning has two discrete dynamics, it is only natural to model it as a switched nonlinear system. The switched nonlinear system:

$$\dot{\boldsymbol{\xi}} = \mathbf{A}_r(\boldsymbol{\xi}) \tag{14}$$

which in case of valve turning, for each $r \in R = \{1, 2\}$, $\mathbf{A}_r : \mathbb{R}^{2n+2} \to \mathbb{R}^{2n+2}$ is a continuous function as shown in (10). The locally absolutely continuous function $\boldsymbol{\xi} : \mathbb{R}_{\geq 0} \to \mathbb{R}^{2n+2}$ that satisfies (14) for $t \in \mathbb{R}_{\geq 0}$, and a piecewise constant function $r : \mathbb{R}_{\geq 0} \to \{1, 2\}$ with a finite amount of discontinuities in each time interval, complete the solution for (14) [22].

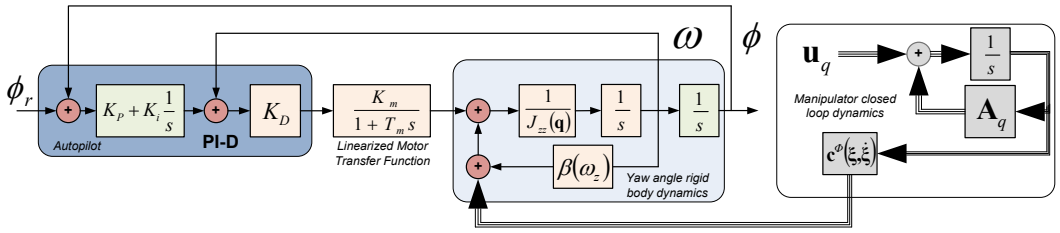

Fig. 4. Yaw angle attitude control system.

For $r = 1$, $\mathbf{A}_r$ is obviously corresponding to (10), has aerodynamic drag $\beta(\omega_z)$, and moment of inertia variations as formulated in (6). When the UAS grabs the valve (i.e. $r = 2$), the system dynamics change: moments of inertia exhibit a discrete event change according to (12); and friction switches from $\beta(\omega_z)$ to equation (13).

IV. Hardware Design and Human Machine Interface (HMI)

We aim to utilize mobile manipulating aerial platforms in a multi-agent system that has the ability to perform both reconnaissance missions and missions that require interaction with its surroundings (Fig. 5). We strongly believe that building such a system raises the need for a completely new human-machine interaction. Although the HMI design goes beyond the scope of this paper, we briefly introduce it in this section to better clarify the procedures we used in our experiments. As shown in Fig. 5, the proposed HMI design requires input both from classical joystick controllers, as well as voice recognition and motion detection.

For the low-level control, an off-the-shelf autopilot is used to control the yaw, pitch, and roll of the quadrotor through gyroscopic sensor data. Integrated with the low-level controller, a high-level autopilot controller using a motion capture system that provides x, y, z position and velocity information is proposed. Motion capture is based on vision markers placed just above the center of mass of the vehicle. A PC-based control station reads an array of commands from multiple inputs (i.e. joystick, motion detection and voice control) to navigate the UAS in the motion tracking volume.

V. Experimental Results

Using the proposed HMI design, an experiment was conducted where an operator navigates the UAS towards the valve, lands on the valve, and grabs it. Before the actual grab, a quadrotor is commanded to different yaw angle set points in order to test the yaw angle controllers. After the grab, the change of setpoints is repeated in order to compare the two responses. The approach and grab are shown in three snapshots shown in Fig. 6.

It is worth noting that the valve used during these experiments differs significantly from standard industrial valves. This explains such a similarity between the results shown in Figs. 7 and 8. The valve exerts friction as shown in (13), but with a lot less static and dynamic friction as it would normally have. Therefore, the biggest contribution to system dynamics comes from changes in moments of inertia and viscous friction. Increases in moments of inertia lowers the open loop gain, thus introducing a larger overshoot, as shown in Fig. 8.

VI. Conclusions

In this paper an arm-aircraft system for valve turning is presented and validated through flight tests. Our experimental results confirm the kinematic and dynamic model and controller for the system. Through a human machine interface, the UAS is commanded to approach, grab, and turn a mock industrial valve. Learning from previous experiments, a single operator flying the aircraft and manipulating objects proved to be extremely difficult. With the proposed HMI, a single operator easily control the UAS through arm motion and voice control. Vehicle performance in terms of stability and robustness to contact forces surpassed expectations.

Future work involves defining additional benchmark missions that could test the performance of the proposed unmanned aerial system. Furthermore, we plan to invest a lot of time to further develop the augmented human-machine interface. We aim to research possibilities to introduce devices and means that would further enhance an operator's capability to interact with the system (hand gestures, pedals, EEG helmet, IMUs, etc.). At the same time, we will provide the HMI with information on the operator state (EKG, skin conductance, HR, breathing rate, etc.), thus allowing the system to autonomously override operator inputs if necessary.

Fig. 5. Human in the loop control of unmanned aerial system using motion detection, voice control, and classical joystick inputs.

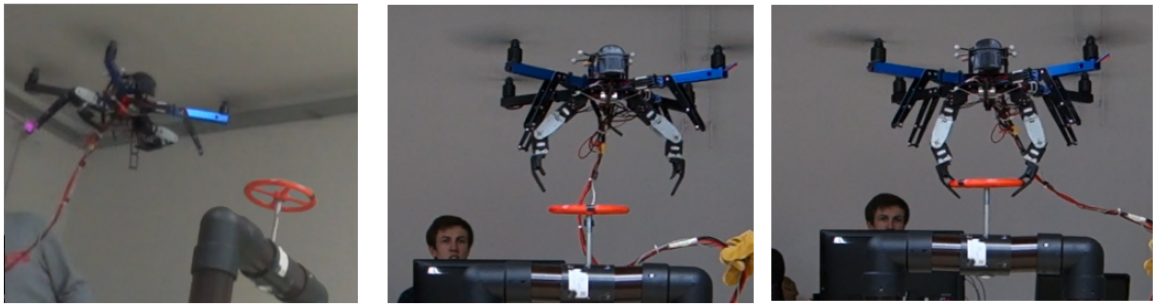

Fig. 6. MMUAV approaching and grabbing a valve: Taking off with arms stowed away for safety; approaching the valve; grabbing the valve.

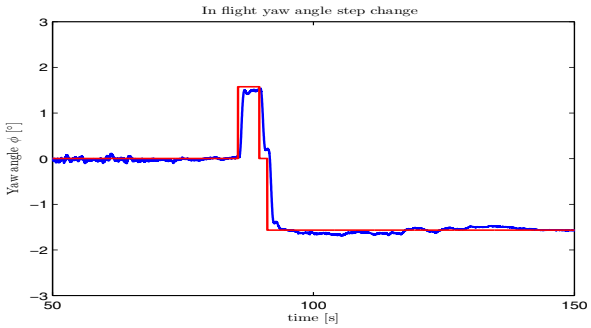

Fig. 7. Yaw angle step response when UAS is grabbing a valve.

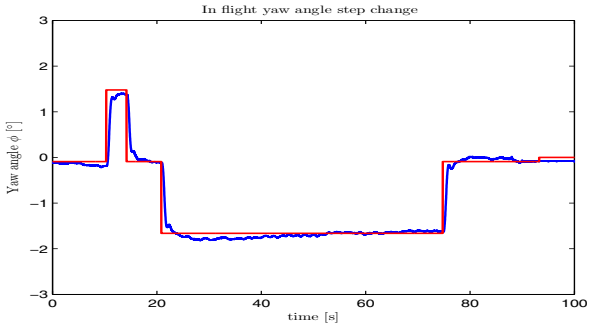

Fig. 8. Yaw angle step response while UAS is flying (no contact with environment).

REFERENCES

[1] S. Kim, S. Choi, and H. J. Kim, "Aerial manipulation using a quadrotor with a two dof robotic arm," in *IEEE/RSJ International Conference on Intelligent Robots and Systems*, Tokyo, Japan, 2013.

[2] F. Huber, K. Kondak, K. Krieger, D. Sommer, M. Schwarzbach, M. Laiacker, I. Kossyk, S. Parusel, S. Haddadin, and A. Albu-Schaffer, "First analysis and experiments in aerial manipulation using fully actuated redundant robot arm," in *IEEE/RSJ International Conference on Intelligent Robots and Systems*, Tokyo, Japan, 2013.

[3] J. Scholten, M. Fumagalli, S. Stramigioli, and R. Carloni, "Interaction control of an uav endowed with a manipulator," in *Robotics and Automation (ICRA), 2013 IEEE International Conference on*, May 2013, pp. 4910–4915.

[4] M. Fumagalli, R. Naldi, A. Macchelli, R. Carloni, S. Stramigioli, and L. Marconi, "Modeling and control of a flying robot for contact inspection," in *Intelligent Robots and Systems (IROS), 2012 IEEE/RSJ International Conference on*, Oct 2012, pp. 3532–3537.

[5] K. Kondak, K. Krieger, A. Albu-Schaeffer, M. Schwarzbach, M. Laiacker, I. M. A. Rodriguez-Castano, and A. Ollero, "Closed-loop behavior of an autonomous helicopter equipped with a robotic arm for aerial manipulation tasks," in *International Journal of Advanced Robotic Systems*, 2013.

[6] A. Jimenez-Cano, J. Martin, G. Heredia, A. Ollero, and R. Cano, "Control of an aerial robot with multi-link arm for assembly tasks," in *Robotics and Automation (ICRA), 2013 IEEE International Conference on*, May 2013, pp. 4916–4921.

[7] V. Lippiello and F. Ruggiero, "Exploiting redundancy in cartesian impedance control of uavs equipped with a robotic arm," in *Intelligent Robots and Systems (IROS), 2012 IEEE/RSJ International Conference on*, 2012, pp. 3768–3773.

[8] I. Palunko and R. Fierro, "Adaptive feedback controller design and quadrotor modeling with dynamic changes of center of gravity," vol. 18, no. 1, August-September 2011, pp. 2626–2631.

[9] C. Korpela, M. Orsag, M. Pekala, and P. Oh, "Dynamic stability of a mobile manipulating unmanned aerial vehicle," in *Robotics and Automation (ICRA), 2013 IEEE International Conference on*, May 2013, pp. 4922–4927.

[10] M. Orsag, C. Korpela, and P. Oh, "Modeling and control of mm-uav: Mobile manipulating unmanned aerial vehicle," *Journal of Intelligent & Robotic Systems*, vol. 69, no. 1-4, pp. 227–240, 2013.

[11] [Online]. Available: http://www.theroboticschallenge.org/

[12] N. Alunni, C. Phillips-Grafftin, H. Suay, D. Lofaro, D. Berenson, S. Chernova, R. Lindeman, and P. Oh, "Toward a user-guided manipulation framework for high-dof robots with limited communication," in *Technologies for Practical Robot Applications (TePRA), 2013 IEEE International Conference on*, April 2013, pp. 1–6.

[13] MIL-STD-101B, "Military standard: Color code for pipelines and for compressed gas cylinders," [Online] Available: http://www.wbdg.org/, 1970.

[14] C. Korpela, M. Orsag, T. Danko, B. Kobe, C. McNeil, R. Pisch, and P. Oh, "Flight stability in aerial redundant manipulators," in *Proc. IEEE Int Robotics and Automation (ICRA) Conf*, 2012.

[15] http://www.dlr.de.

[16] M. Orsag, C. Korpela, S. Bogdan, and P. Oh, "Hybrid adaptive control for aerial manipulation," *Journal of Intelligent and Robotic Systems*, vol. 73, no. 1-4, pp. 693–707, 2014. [Online]. Available: http://dx.doi.org/10.1007/s10846-013-9936-1

[17] C. M. Korpela, T. W. Danko, and P. Y. Oh, "Designing a system for mobile manipulation from an unmanned aerial vehicle," in *Proc. IEEE Conf. Technologies for Practical Robot Applications (TePRA)*, 2011, pp. 109–114.

[18] ——, "MM-UAV: Mobile manipulating unmanned aerial vehicle," *Journal of Intelligent and Robotic Systems*, vol. 65, no. 1-4, pp. 93–101, 2012.

[19] G. M. Hoffmann, H. Huang, S. L. Wasl, and E. C. J. Tomlin, "Quadrotor helicopter flight dynamics and control: Theory and experiment," in *In Proc. of the AIAA Guidance, Navigation, and Control Conference*, 2007.

[20] R. E. Mahony, V. Kumar, and P. Corke, "Multirotor aerial vehicles: Modeling, estimation, and control of quadrotor," *IEEE Robot. Automat. Mag.*, pp. 20–32, 2012.

[21] R. Schilling, *Fundamentals of robotics: analysis and control*. Prentice Hall, 1990. [Online]. Available: http://books.google.hr/books?id=LcxSAAAAMAAJ

[22] J. Hespanha, "Uniform stability of switched linear systems: extensions of lasalle's invariance principle," *Automatic Control, IEEE Transactions on*, vol. 49, no. 4, pp. 470–482, April 2004.